

## Magnetotransport behavior of polycrystalline $\text{YBa}_2\text{Cu}_3\text{O}_7$ : A possible role for surface barriers

Shi Li, M. Fistul, J. Deak, P. Metcalf, G. F. Giuliani, and M. McElfresh  
*Physics Department, Purdue University, West Lafayette, Indiana 47907*

D. L. Kaiser

*Ceramics Division, National Institute of Standards and Technology, Gaithersburg, Maryland 20899*

(Received 19 December 1994)

The magnetization as a function of external applied magnetic field  $M(H_{\text{ext}})$  of polycrystalline  $\text{YBa}_2\text{Cu}_3\text{O}_7$  (poly-YBCO) exhibits behavior that is more consistent with the geometrical barrier model of Zeldov *et al.* than that of either the Bean-Livingston surface-barrier model or the Bean critical state strong-pinning model. Correlation of the magnetization measurements with transport measurements suggests that the irreversible properties of poly-YBCO, including the critical current density  $J_c$ , are dominated by surface-barrier effects. Observation of an increasing of  $J_c$  with  $H_{\text{ext}}$  at intermediate fields is consistent with a theoretical model that describes the transport behavior in the case of vortex lattice formation within the superconducting grains that form the Josephson junctions.

Recently, there have been numerous reports describing evidence of surface barriers in high-temperature superconductors.<sup>1</sup> While surface barriers may be present under strong flux-pinning conditions, surface-barrier behavior is usually only evident in regimes where flux pinning is weak. For both bulk and powdered polycrystalline  $\text{YBa}_2\text{Cu}_3\text{O}_7$  (poly-YBCO), the magnetization as a function of externally-applied magnetic field  $M(H_{\text{ext}})$  exhibits a behavior that is more consistent with either the Bean-Livingston<sup>2</sup> (BL) or geometrical<sup>3</sup> surface-barrier models than it is with the Bean critical state model.<sup>4</sup> While poly-YBCO has a complex microstructure consisting of crystalline grains, grain boundaries, and voids, it is quite possible that the individual crystallites in well-annealed fully-oxygenated poly-YBCO are actually low-defect-density crystals. Thus the irreversible properties of poly-YBCO, including the magnitude of the critical current density  $J_c$ , may be dominated by surface-barrier effects rather than by strong pinning at defects. In addition to the  $M(H_{\text{ext}})$  behavior, the anomalous increase of  $J_c$  with external applied field  $H_{\text{ext}}$ ,<sup>5</sup> that is observed at intermediate fields, is consistent with weak pinning and the formation of an ordered vortex lattice inside the individual grains.<sup>6</sup>

The simplest description of granular superconductors considers the material to be an ensemble of superconducting grains connected by weak links.<sup>7</sup> Within this description the critical current  $I_c$  of the whole structure is determined by the Josephson currents flowing between the grains. The grain boundaries in poly-YBCO, as well as in the other polycrystalline CuO-based high-temperature superconducting materials, behave like superconducting weak links. This has been demonstrated in many studies of individual grain boundaries in which a variety of variables were controlled.<sup>8,9</sup> Many other studies of polycrystalline materials support this conclusion.<sup>10</sup>

When a small external magnetic field  $H_{\text{ext}}$  (i.e.,  $H_{\text{ext}} \ll H_{pJ}$ , the field of initial intragranular penetration) is applied to a granular superconductor, the magnetic field penetrates into both the intergranular regions of the material and

the surface of each grain. The resulting surface layer in the grains has an average thickness determined by the London penetration depth  $\lambda_L$ . Associated with this surface penetration is a shielding current  $j_M$  [see Fig. 1(a)]. For a single small Josephson junction of length  $L$ , the dependence of the critical current on an external magnetic field  $I_c(H_{\text{ext}})$  is simply given by the familiar Fraunhofer dependence

$$I_c(H_{\text{ext}}) = I_c(0) \left| \frac{\sin(\pi \phi_{\text{ext}} / \phi_0)}{(\pi \phi_{\text{ext}} / \phi_0)} \right|, \quad (1)$$

where  $\phi_{\text{ext}} = 2\lambda_L L H_{\text{ext}}$  is the approximate total magnetic flux threading the junction,<sup>11</sup>  $I_c(0)$  is the critical current in zero applied field, and  $\phi_0$  the flux quantum. In the polycrystalline material, however, this simple situation for a single Josephson junction must be modified to account for the complicated connectivity of the granular structure. An important feature of this granular structure is the broad distribution of grain sizes, and therefore junction sizes, as well as the local critical currents. This distribution results in different amounts of flux threading the numerous effective junctions, which leads to an averaging out of the oscillatory contributions to the global  $I_c(H_{\text{ext}})$  and a monotonic decrease of the critical current with  $H_{\text{ext}}$ . In particular, using a grain-size distribution that is a constant up to sizes of the order of  $\phi_0 / \lambda_L H_{\text{ext}}$ , calculations have shown that  $I_c(H_{\text{ext}})$  behaves approximately as  $I_c(H_{\text{ext}}) \sim 1/H_{\text{ext}}$ .<sup>12</sup> Thus prior to intragranular flux penetration into the grains,  $j_M$  is proportional to  $H_{\text{ext}}$  so that  $I_c$  is inversely proportional to  $j_M$ .

For sufficiently large external magnetic fields ( $H_{\text{ext}} > H_{pG}$ ) Abrikosov vortices will penetrate into the superconducting grains. When the flux pinning is strong, or the system is at temperatures above a lattice-melting-type transition temperature  $T_m$ , the spatial distribution of these vortices will be random. However, in the case of weak bulk pinning at temperatures below  $T_m$ , the vortices can actually form an ordered lattice. The penetration of vortices to form an ordered lattice within the grains produces a current contribution  $j_{AV}$  that cancels a portion of the Meissner current  $j_M$  near the boundary between two grains [see Fig. 1(b)].<sup>6,13</sup>

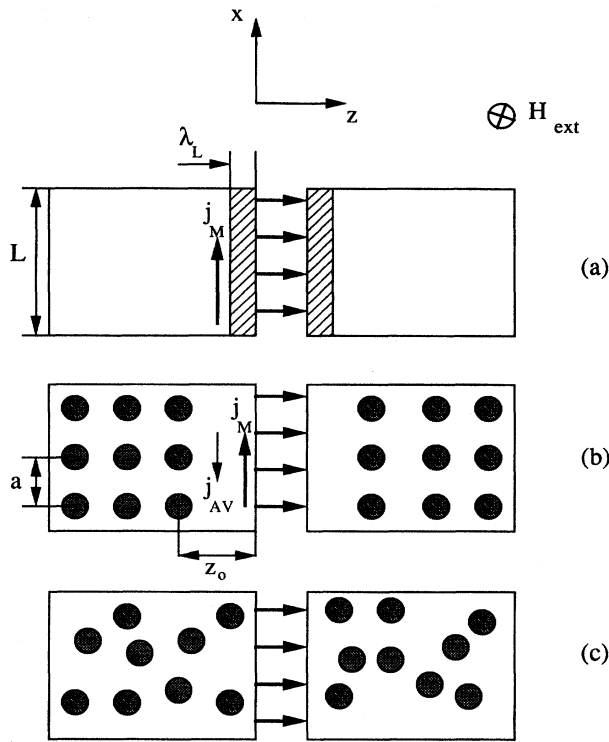


FIG. 1. Schematic diagram showing the effects of an externally applied magnetic field on a Josephson junction having a length  $L$ . (a) At  $H_{\text{ext}} < H_{pG}$ , the field penetrates the surface of the grains to a depth  $\lambda_L$ , the London penetration depth, and a current  $j_M$  is induced at the surface of the junction. (b) For the case of weak pinning at  $T < T_m$  (flux lattice melting transition) and  $H_{\text{ext}} > H_{pG}$ , flux penetrates the grains to form an ordered lattice having a lattice constant  $a$ . A current  $j_{AV}$  is induced near the surface of the junction which partially cancels  $j_M$ . The distance of the lattice from the junction surface,  $z_0$ , affects the value of  $j_{AV}$ . (c) For the case  $H_{\text{ext}} > H_{pG}$  and either  $T > T_m$  or pinning is strong, flux penetrates the grains to form a random distribution of vortices. The random distribution does not produce an efficient cancellation of  $j_M$ .

In the case of random vortex arrangements, however, the additional current contribution is distributed randomly resulting in little cancellation of  $j_M$  near the surface. Since  $I_c$  is inversely proportional to the total current near the junction surface, a more effective cancellation of  $j_M$  will allow a higher critical current to flow between the grains (across the junction). Thus the formation of an ordered lattice of vortices can actually reverse the decrease of  $I_c$  with  $H_{\text{ext}}$  and result in an increase in  $I_c$ . In contrast to this, for the case of a random arrangement of vortices upon penetration, a decrease of  $I_c$  is expected.

In Ref. 6 the dependence of  $I_c$  on  $H_{\text{ext}}$  for a Josephson junction having a stationary (constrained) ordered lattice of Abrikosov vortices with a particular geometrical arrangement was calculated. The main results can be cast in the form,

$$I_c(H_{\text{ext}}) \approx I_c(0) / \{|M_G| + \alpha H_{\text{ext}}\}, \quad (2)$$

where  $M_G$  is the total magnetization of a superconducting grain and  $\alpha = [z_0 - (a/2)] / 8\pi\lambda_L$ . Here  $a$  is the vortex lattice parameter and  $z_0$  is the distance from the nearest vortex line to the junction surface [see Fig. 1(b)]. Thus the  $I_c(H_{\text{ext}})$  dependence is expected to become weaker with the increasing extent of flux penetration. Furthermore, over a wide range of magnetic fields the critical current can actually increase with  $H_{\text{ext}}$  as observed in the experiments described below. This behavior is in contrast to the case of strong bulk pinning where the vortices penetrate the grains in a disordered fashion. A previous study demonstrated that, for strong pinning, one expects the critical current to behave like  $(H_{\text{ext}})^{-1/4}$  (Ref. 14).

For these studies, a nearly randomly-oriented poly-YBCO specimen was synthesized using standard ceramic preparation methods.<sup>15</sup> The desired average grain size and density was attained by using known temperature-time profiles for environments in which the oxygen partial pressure was carefully controlled.<sup>16</sup> The resulting material had a density of about 81% of the theoretical value, a median grain size of 8  $\mu\text{m}$ , a superconducting transition temperature  $T_c = 91$  K, and a transition width  $\Delta T_c$  of about 2 K was measured by ac susceptibility at 2.5 MHz. The YBCO single crystal used for comparative purposes had a  $T_c = 93$  K. It was grown from a Y-Ba-Cu-O melt using a technique described elsewhere;<sup>17</sup> a thermomechanical process was used to remove the twin boundaries.<sup>18</sup>

The externally applied field dependence of the bulk magnetization  $M(H_{\text{ext}})$  was measured using a Quantum Design superconducting quantum interference device magnetometer after cooling the specimen in zero field. A standard four-point probe technique<sup>19</sup> was used to measure the electric field as a function of current density  $E(J)$  at various fields and temperatures. A  $1.7 \times 10^{-8}$  V/cm  $E$ -field criterion was used to determine  $J_c$  from the  $E(J)$  curves, however, only  $E(J)$  curves with negative curvature were considered suitable for this determination.

The shape of the  $M(H_{\text{ext}})$  loop in Fig. 2 more closely resembles the  $M(H_{\text{ext}})$  curve for a system exhibiting surface barrier (i.e., BL or geometrical) behavior<sup>2,3</sup> than one exhibiting Bean critical-state behavior.<sup>4</sup> For poly-YBCO, Bean-like  $M(H)$  loops have been observed at low temperatures and also for neutron irradiated material.<sup>20</sup> However, the present poly-YBCO specimen shows only barrierlike  $M(H_{\text{ext}})$  behavior down to the lowest temperature studied ( $T = 10$  K). As a comparison, the  $M(H_{\text{ext}})$  behavior for a detwinned YBCO single crystal is shown in Fig. 3. For both the poly-YBCO specimen and the single crystal, the observed behavior is most consistent with the geometrical behavior model: on decreasing the magnetic field,  $M$  is finite over a wide range of fields. In this model, first flux penetration into the grains occurs initially at  $H_{pG} = 4\pi H_{c1}(w/d)^{1/2}$ , where  $H_{c1}$  is the lower critical field,  $w$  is the width, and  $d$  is the thickness of the crystal in a plane perpendicular to the direction of the applied field. In addition, as  $H_{\text{ext}}$  is decreased from above  $H_{pG}$ , the surface-barrier model predicts that  $M = 4\pi H_{c1}$ . This result is in contrast to that predicted by the BL barrier model where  $M$  is expected to vanish over a wide range when  $H_{\text{ext}}$  decreases from above  $H_{pG}$ .

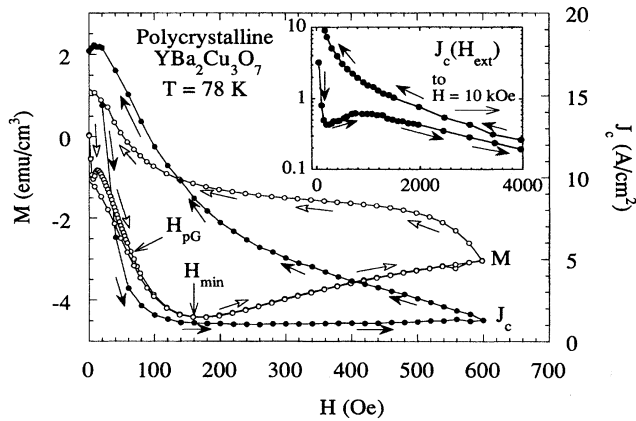


FIG. 2. Magnetization as a function of external applied field  $M(H_{\text{ext}})$  (open circles) and transport measurement determinations of the critical current density  $J_c$  as a function of applied magnetic field  $J_c(H_{\text{ext}})$  (filled circles) at  $T = 78$  K.  $H_{pG}$  identifies the point at which flux begins to penetrate into the individual grains, while  $H_{\text{min}}$  identifies the coincident point where  $M$  begins to decrease and  $J_c$  actually begins to increase with  $H_{\text{ext}}$ . The inset shows a typical case of  $J_c(H_{\text{ext}})$  measured at larger field values.

The  $M(H_{\text{ext}})$  behavior of the poly-YBCO specimen is also consistent with the behavior expected for a granular superconductor.<sup>7</sup> At small magnetic fields,  $0 < H_{\text{ext}} < 8$  Oe, the sample exhibits complete shielding of the bulk suggesting that the magnetic field only penetrates a distance  $\lambda$ , the penetration depth, near the surface of the bulk sample (region I). When the field increases to values within the range  $8 \text{ Oe} < H_{\text{ext}} < 150$  Oe, the magnetic field penetrates between the grains but Abrikosov vortices are not present inside the grains (region II). A further increase of the external field ( $H_{\text{ext}} > H_{pG}$ ) leads to the creation of vortices inside the grains. At sufficiently high fields ( $H_{\text{ext}} > H_{\text{min}}$ ), the total magnetization decreases. The slope  $\chi_i$  of the  $M(H_{\text{ext}})$  in regions I ( $\chi_I$ ) and II ( $\chi_{II}$ ) can be described by

$$M = \chi_i H_{\text{ext}}, \quad \chi_I = -(1/4\pi)\rho,$$

$$\chi_{II} = -(1/4\pi)\rho[1 - (4\lambda_L/L)],$$

where the parameter  $\rho$  characterizes the density of the material (here,  $\rho \approx 0.8$ ). A value  $\lambda_L \approx 6000$  Å can be determined using the value  $\chi_{II} = -0.0446 \text{ emu/cm}^3 \text{ Oe}$  determined from Fig. 2 and the mean grain size  $L \approx 8 \mu\text{m}$ . This value for  $\lambda_L$  falls between the upper and lower limits ( $\lambda_{ab} \sim 2000$  Å and  $\lambda_c \sim 11\,000$  Å) at  $T = 78$  K previously reported for the various crystallographic orientations of YBCO.<sup>21</sup>

As seen in Fig. 2, a plateau in  $M(H_{\text{ext}})$  is observed when the external magnetic field is reduced. A nearly constant value of the total magnetization is observed over the range  $200 \text{ Oe} < H_{\text{ext}} < 500$  Oe when the field is reduced from  $H_{\text{ext}} = 600$  Oe. Measurements extending to higher fields show that a plateau is reached after decreasing the field by about 100 Oe. A similar plateau is observed for the detwinned single crystal; however, the curvature immediately after field reduction is quite different from that of the polycrystalline specimen, with a plateau reached after a field reduction of only a few Oe. This behavior for the poly-YBCO specimen is consistent with the case of a surface barrier at the grain boundary and no (or very weak) bulk pinning inside the grains. For a BL surface barrier, the vortices initially remain in the grains after the field is reduced if a surface barrier is present. However, after a sufficient reduction of the field, the BL barrier will vanish and vortices will leave the sample; the magnetization will then decrease to zero. One possible explanation for the nonzero  $M$  value evident in Fig. 2 is that there is a difference between the external field and the actual distribution of the magnetic field between the grains that results from the residual magnetization of the Josephson media. Another explanation is that each grain behaves like a distinct system exhibiting geometrical barrier behavior. The latter explanation is supported by comparative measurements that show there is little difference between the

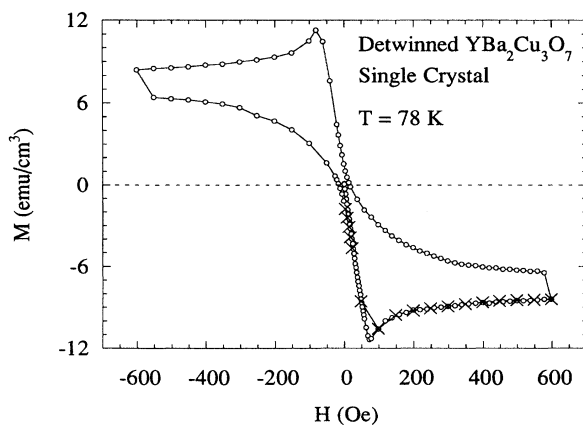


FIG. 3. Magnetization as a function of external applied field  $M(H_{\text{ext}})$  for a detwinned single crystal of YBCO at  $T = 78$  K. The observed behavior is more consistent with that of the geometrical barrier model than either the Bean-Livingston surface-barrier model or the Bean critical state model of strong flux pinning.

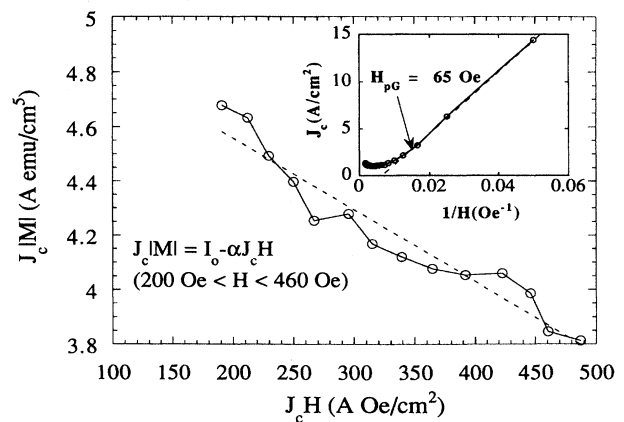


FIG. 4. A plot of  $J_c|M|$  as a function of  $J_c H_{\text{ext}}$  for fields above  $H_{pG}$  ( $200 \text{ Oe} < H_{\text{ext}} < 460$  Oe). The small slope value  $\alpha = -2.6 \times 10^{-3}$  suggests that  $z_0 - a/2 \ll a$  and that grains which contribute most strongly to the observed transport  $J_c$  have a nearly ideal vortex-lattice positioning across connected grains. The inset shows that  $J_c \sim 1/H_{\text{ext}}$  prior to flux penetration into the grains.

$M(H_{\text{ext}})$  curves of bulk and powdered poly-YBCO specimens except at low  $H_{\text{ext}}$  values.<sup>22</sup>

The specific dependence of  $I_c(H_{\text{ext}})$  can be correlated quantitatively with the  $M(H_{\text{ext}})$  behavior using Eq. (2), which describes the  $I_c$  behavior in the case of no bulk pinning. At small magnetic fields  $H_{\text{ext}} < H_{pG}$ , Abrikosov vortices do not penetrate into the grains and flux compression is very large outside of the grains. The critical current is then determined by the Josephson current between adjacent grains and has the approximate dependence  $I_c \cong H_{\text{ext}}^{-1}$ . This dependence is consistent with the results of Fig. 2 as plotted in the form shown in the inset of Fig. 4. When Abrikosov vortices penetrate into the grains at  $H_{\text{ext}} = H_{pG}$ , the critical current density  $J_c$  becomes more weakly dependent on  $H_{\text{ext}}$ , as also seen in Fig. 2. For a Josephson junction with an ordered array of vortices,  $I_c$  is given by Eq. (2). Figure 4 is a plot of  $J_c |M|$  as a function of  $J_c H_{\text{ext}}$  for fields above  $H_{pG}$  (200 Oe  $< H_{\text{ext}} < 460$  Oe). The fit (dashed line) is done assuming a constant value for the slope  $\alpha$  in Eq. (2). The value  $\alpha = -2.6 \times 10^{-3}$  is rather small implying that  $z_0 - a/2 \ll a$ . This is consistent with an ideal positioning of parallel vortex lines across the junction barriers (i.e.,  $z_0 \sim a/2$ ). This suggests that it is grains of this kind which contribute most

strongly to the observed transport  $J_c$ . This symmetric configuration is also consistent with a large suppression of the currents near the surface ( $j_M$ ) and can account for the observed increase in  $J_c$  at intermediate fields.

In summary, the shape of the  $M(H_{\text{ext}})$  for poly-YBCO, both bulk and powdered, is very similar to that of a high-quality detwinned single crystal of YBCO. This shape is characteristic of surface barrier rather than strong pinning behavior, with the nonzero  $M$ , observed on reduction of  $H_{\text{ext}}$  in all cases, being more consistent with the geometrical surface-barrier model. The upturn in  $J_c$  observed at intermediate  $H_{\text{ext}}$  is consistent with the formation of an ordered lattice within the individual grains which requires very weak pinning to exist within the grains. These results suggest that the irreversibility and resulting  $J_c$  of poly-YBCO is due to surface-barrier effects rather than bulk pinning at defects.

We would like to thank S. Gerber, M. Konczykowski, H. Nakanishi, and E. Zeldov for valuable discussions and M. Darwin for technical assistance. The work of Purdue University was supported by the Director for Energy Research, Office of Basic Energy Sciences through the Midwest Superconductivity Consortium (MISCON) DOE Grant No. DE-FG02-90ER45427.

- 
- <sup>1</sup>M. Konczykowski, L. I. Burlachkov, Y. Yeshurun, and F. Holtzberg, *Phys. Rev. B* **43**, 13 707 (1991).
- <sup>2</sup>C. P. Bean and J. D. Livingston, *Phys. Rev. Lett.* **12**, 14 (1964).
- <sup>3</sup>E. Zeldov, A. I. Larkin, V. B. Geshkenbein, M. Konczykowski, D. Majer, B. Khaykovich, V. M. Vinokur, and H. Shtrikman, *Phys. Rev. Lett.* **73**, 1428 (1994).
- <sup>4</sup>C. P. Bean, *Rev. Mod. Phys.* **36**, 31 (1964).
- <sup>5</sup>J. R. Thompson, J. Brynstad, D. M. Kroeger, Y. C. Kim, S. T. Sekula, D. K. Christen, and E. D. Specht, *Phys. Rev. B* **39**, 6652 (1989); L. M. Fisher, N. V. Il'in, N. A. Podlevskikh, S. I. Zakharchenko, *Solid State Commun.* **73**, 687 (1990).
- <sup>6</sup>M. Fistul and G. F. Giuliani, *Phys. Rev. B* **51**, 1090 (1995).
- <sup>7</sup>J. E. Evetts and B. A. Glowacki, *Cryogenics* **28**, 641 (1988).
- <sup>8</sup>S. E. Babcock and D. C. Larbalestier, *J. Appl. Phys.* **55**, 393 (1989).
- <sup>9</sup>D. Dimos, P. Chaudhari, and J. Mannhart, *Phys. Rev. B* **41**, 4038 (1990).
- <sup>10</sup>S. E. Babcock, T. F. Kelly, P. J. Lee, J. M. Seuntjens, L. A. Lavanier, and D. C. Larbalestier, *Physica C* **152**, 25 (1988).
- <sup>11</sup>A. Barone and G. Paterno, *Physics and Applications of the Josephson Effect* (Wiley, New York, 1982).
- <sup>12</sup>E. Z. Meilixov and U. V. Gershanov, *Physica C* **157**, 431 (1989).
- <sup>13</sup>M. Fistul and G. F. Giuliani, *Physica C* **230**, 9 (1994).
- <sup>14</sup>M. V. Fistul, *JETP Lett.* **49**, 116 (1989).
- <sup>15</sup>T. Schuster, M. R. Koblischaka, B. Ludescher, R. Henes, A. Kottmann, and H. Kvonmuller, *Mater. Lett.* **14**, 189 (1992).
- <sup>16</sup>J. P. Singh, R. A. Guttschow, J. T. Dusek, and R. B. Poeppel, *J. Mater. Res.* **7**, 2324 (1992).
- <sup>17</sup>D. L. Kaiser, F. Holtzberg, B. A. Scott, and T. R. McGuire, *Appl. Phys. Lett.* **51**, 1040 (1987); D. L. Kaiser, F. Holtzberg, M. F. Chisholm, and T. K. Worthington, *J. Cryst. Growth* **85**, 593 (1987).
- <sup>18</sup>D. L. Kaiser, F. W. Gayle, R. S. Roth, and L. J. Swartzendruber, *J. Mater. Res.* **4**, 745 (1989).
- <sup>19</sup>J. Deak, M. McElfresh, J. R. Clem, Z. Hao, M. Konczykowski, R. Muenchausen, S. Foltyn, and R. Dye, *Phys. Rev. B* **47**, 8377 (1993).
- <sup>20</sup>H. S. Lessure, S. Simizu, B. A. Baumert, S. G. Sankar, and M. E. McHenry, *IEEE Trans. Magn.* **27**, 1043 (1991).
- <sup>21</sup>L. Krusin-Elbaum, R. L. Greene, F. Holtzberg, A. P. Malozemoff, and Y. Yeshurun, *Phys. Rev. Lett.* **62**, 217 (1989).
- <sup>22</sup>S. Li, M. Fistul, J. Deak, P. Metcalf, and M. McElfresh, *Phys. Rev. B* **52**, R747 (1995).